Polymer Chemistry

Cite this: *Polym. Chem.*, 2011, **2**, 1815

www.rsc.org/polymers

PAPER

Self-association behavior in water of an amphiphilic diblock copolymer comprised of anionic and dendritic blocks

Shin-ichi Yusa,*[a] Yoshihiko Shimada,[a] Toyoko Imae[b] and Yotaro Morishima[c]

Received 16th March 2011, Accepted 27th April 2011
DOI: 10.1039/c1py00111f

Well-defined amphiphilic diblock copolymers (PAMPS-*b*-PG2) composed of a hydrophilic linear polyelectrolyte and hydrophobic blocks bearing pendent dendritic moieties was synthesized *via* reversible addition–fragmentation chain transfer (RAFT) controlled radical polymerization of 3,5-bis [3′,5′-bis(benzyloxy)benzyloxy]benzyl 11-acrylamidoundecanoate (G2) using a poly(sodium 2-(acrylamido)-2-methylpropanesulfonate) (PAMPS) based macro-chain transfer agent. Degrees of polymerization of PAMPS and PG2 blocks were 71 and 3, respectively. The polydispersity index was 1.25 as estimated from GPC. Hydrophobic association of the PG2 blocks in aqueous solutions was suggested from restricted motions of the dendritic moieties as observed by ^{1}H NMR in D_2O. A fluorescence spectrum of 8-anilino-1-naphthalenesulfonic acid, ammonium salt hydrate indicated that the fluorescence probe was solubilized in the hydrophobic domain formed from the polymer aggregate in water. The formation of polymer aggregates was indicated by light scattering data. The hydrodynamic radius (R_h) of the polymer aggregate was independent of the polymer concentration.

Introduction

It is well established that amphiphilic block copolymers form micelles where hydrophobic sequences constitute cores and hydrophilic sequences form shells.[1] Considerable attention, both from scientific and technological points of view, has been focused on amphiphilic block copolymer micelles because they are expected to be a potentially useful material for practical applications such as drug delivery,[2–4] separation,[5] and catalysis.[6]

Dendrimers, including hyperbranched macromolecules, with a tailor made structure have been investigated as attractive compounds for various fields such as nano-scale reactors, diagnostics, gene delivery vectors, magnetic resonance imaging agents, and homogeneous catalysts.[7,8] Furthermore, dendrimers are ideal building blocks for polymer architecture, because their structure can be controlled precisely. Xi *et al.*[9] reported synthesis of methacrylates with a dendritic moiety as a pendent group and their radical polymerization. Stupp and Zubarev[10] reported synthesis of a series of triblock structures containing dendritic, rodlike, and coillike blocks by a combination of anionic polymerization and step-by-step condensation reactions. Fréchet *et al.*[11–13] reported the synthesis and association behavior of linear poly(ethylene oxide)-dendritic benzyl ether amphiphilic block copolymers. Imae *et al.*[14] also reported the preparation and physicochemical properties of amphiphilic polymers including dendritic moiety. The large degree of vacancies in the interior of dendrons offers the ability to encapsulate many guest molecules. Their numerous end groups can be modified with various chemical functional groups.

In the past decade, the development of the controlled radical polymerization methods allows the synthesis of a wide variety of block copolymers under mild conditions. Nitroxide-mediated or stable free radical polymerization (SFRP),[15] atom transfer radical polymerization (ATRP),[16,17] and reversible addition–fragmentation chain transfer (RAFT) radical polymerization[18] are the most studied methods. These methods are based on a reversible activation/deactivation cycle of propagating polymer radicals, resulting in a small fraction of propagating polymer radicals and a large fraction of reversible deactivated dormant polymer chains. The low concentration of active propagating polymer radicals suppresses possible termination and side reactions. Recently, well defined linear-dendritic block copolymers are prepared by SFRP[19,20] and ATRP.[21]

Among the available controlled radical polymerization methods, RAFT polymerization is applicable to a wide range of monomers, functional groups, and reaction conditions including aqueous media. The RAFT process is achieved simply by the addition of a suitable chain transfer agent (CTA) to an ordinary radical polymerization system. The polymers obtained by the RAFT process can be used as precursors to block copolymers by the addition of further monomer. From these advantages, many research groups have focused on the employment of the RAFT process in the controlled polymerization.[21–24]

[a]*Department of Materials Science and Chemistry, Graduate School of Engineering, University of Hyogo, 2167 Shosha, Himeji, Hyogo, 671-2201, Japan. E-mail: yusa@eng.u-hyogo.ac.jp; Fax: +81 79 266 8868; Tel: +81 79 267 4954*
[b]*Graduate Institute of Engineering, Jing-Cheng Honors College, National Taiwan University of Science and Technology, 43, section 4, Keelung Road, Taipei, 10607, Taiwan. E-mail: imae@mail.ntust.edu.tw*
[c]*Faculty of Engineering, Fukui University of Technology, 6-3-1 Gakuen, Fukui, 910-8505, Japan. E-mail: morisima@fukui-ut.ac.jp*

In this paper, we report the controlled synthesis of an AB diblock copolymer (PAMPS-*b*-PG2, Fig. 1) of sodium 2-(acrylamido)-2-methylpropanesulfonate (AMPS) and a methacrylamide-based dendritic monomer by the RAFT process using an PAMPS macro-chain transfer agent (macro-CTA). The association behavior of the amphiphilic diblock copolymer in water was characterized with ^{1}H NMR, fluorescence, dynamic light scattering (DLS), static light scattering (SLS), and transmission electron microscopy (TEM) techniques.

Experimental

Materials

4-Cyanopentanoic acid dithiobenzoate was synthesized according to the method reported by McCormick and co-workers.[25] Poly(sodium 2-(acrylamido)-2-methylpropanesulfonate) macro-chain transfer agent (PAMPS macro-CTA) was prepared by RAFT radical polymerization using 4-cyanopentanoic acid dithiobenzoate as a CTA.[25,26] Sodium 11-acrylamidoundecanoate was prepared according to the method of Gan and co-workers.[27] 3,5-Bis[3′,5′-bis(benzyloxy)benzyloxy]benzyl bromide (>98%) from Tokyo Kasei Kogyo Co., 8-anilino-1-naphthalenesulfonic acid, ammonium salt hydrate (97%) (ANS) from Aldrich, and 4,4′-azobis-4-cyanovaleric acid (98%) from Wako Pure Chemicals Co. were used as received without further purification. Dimethylsulfoxide (DMSO) was dried over 4 Å molecular sieves and distilled under reduced pressure. Water was purified with a Millipore Milli-Q system. Other reagents were used as received.

Synthesis of 3,5-bis[3′,5′-bis(benzyloxy)benzyloxy]benzyl 11-acrylamidoundecanoate (G2)

Sodium 11-acrylamidoundecanoate (3.10 g, 11.2 mmol), 3,5-bis[3′,5′-bis(benzyloxy)benzyloxy]benzyl bromide (3.06 g, 3.79 mmol), tetra-*n*-butylammonium bromide (234 mg, 0.744 mmol), and 2,6-di-*tert*-butylcresol (18.5 mg, 0.0840 mmol) in a mixture of water (40 cm^3) and chloroform (20 cm^3) were heated to 110–115 °C in an oil bath for 24 h. The reaction mixture was diluted with chloroform (300 cm^3), washed gently twice with water, and the organic layer was dried over anhydrous sodium sulfate. The solvent was removed by evaporation, and the crude product was purified by silica-gel column chromatography with chloroform as an eluent. The first fraction was collected, and condensation gave a white solid (G2); yield 2.69 g (72.4%); mp 50–51 °C. ^{1}H NMR (500 MHz, $CDCl_3$): δ = 1.12–1.36 (m, 12H, CH_2), 1.41–1.58 (m, 2H, CH_2), 1.59–1.72 (m, 2H, CH_2), 2.32–2.41 (t, 2H, CH_2), 3.24–3.35 (q, 2H, CH_2), 4.97 (s, 4H, CH_2), 5.04 (s, 8H, CH_2), 5.05 (s, 2H, CH_2), 5.52–5.60 (bs, 1H, CON*H*), 5.60–5.66 (m, 1H, vinyl C*H*), 6.01–6.11 (m, 1H, vinyl C*H*), 6.22–6.30 (m, 1H, vinyl C*H*), 6.55 (s, 1H, Ar C*H*), 6.59 (s, 4H, Ar C*H*), 6.69 (s, 4H, Ar C*H*), 7.29–7.48 (m, 20H, Ar C*H*). ^{13}C NMR (DEPT) (126 MHz, $CDCl_3$): δ = 25.04 (*C*H$_2$), 27.03 (*C*H$_2$), 29.22 (*C*H$_2$), 29.33 (*C*H$_2$), 29.37 (*C*H$_2$), 29.47 (*C*H$_2$), 29.55 (*C*H$_2$), 29.65 (*C*H$_2$), 34.39 (*C*H$_2$), 39.71 (*C*H$_2$), 65.97 (*C*H$_2$), 70.07 (*C*H$_2$), 70.19 (*C*H$_2$), 101.67 (Ar *C*H), 101.75 (Ar *C*H), 106.50 (Ar *C*H), 107.14 (Ar *C*H), 126.10 (vinyl *C*H$_2$), 127.66 (Ar *C*H), 128.13 (Ar *C*H), 128.70 (Ar *C*H), 131.17 (vinyl *C*H), 136.86 (Ar *C*), 138.58 (Ar *C*), 139.29 (Ar *C*), 160.09 (Ar *C*), 160.28 (Ar *C*), 165.61 (*C*ONH), 173.71 (*C*OO).

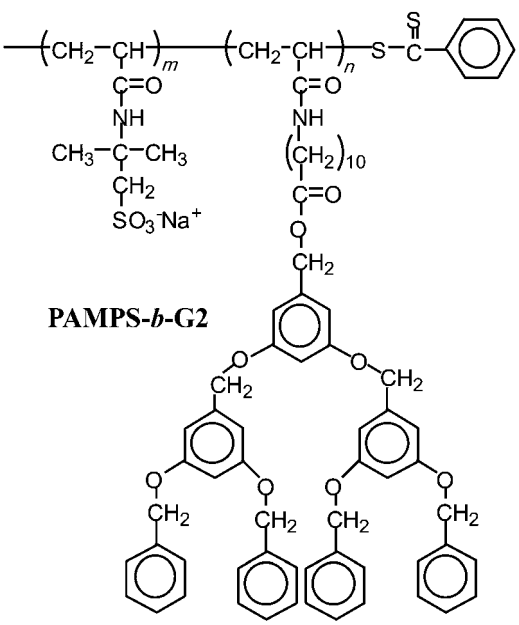

Fig. 1 Chemical structure of PAMPS-*b*-PG2.

Preparation of block copolymers (PAMPS-*b*-PG2)

DMSO was used as solvent for the polymerization to proceed in a homogeneous solution. A typical procedure for the block copolymerization of G2 by the RAFT process is as follows: PAMPS macro-CTA (1.57 g, 0.0709 mmol, M_w (SLS) = 2.21 × 10^4, M_w/M_n (GPC) = 1.28), G2 (2.00 g, 2.04 mmol), and 4,4′-azobis-4-cyanovaleric acid (3.96 mg, 0.0141 mmol) were dissolved in DMSO (25 cm^3). The solution was degassed by Ar bubbling for 30 min. Polymerization was carried out at 70 °C for 24 h. A clear solution of the reaction mixture was poured into a large excess of chloroform to precipitate resulting polymer. The polymer was purified by reprecipitating from a methanol solution into a large excess of chloroform and collected by filtration; yield 0.88 g.

Characterization

GPC. GPC analysis was performed with JASCO GPC-900 equipped with a refractive index (RI) detector and a Shodex 7.0 μm-bead-size GF-7M HQ column (molecular weight range of 10^7 to 10^2) working at 40 °C under a flow rate of 0.6 cm^3 min^{-1}. A methanol solution containing 0.2 M $LiClO_4$ was used as an eluent. The number-average molecular weight (M_n) and molecular weight distribution (M_w/M_n) for the sample polymers were calibrated with standard poly(ethylene oxide) (PEO) samples of eight different molecular weights ranging from 9.60 × 10^2 to 1.01 × 10^5 with narrow M_w/M_n (<1.17).

NMR. ^{1}H NMR spectra were obtained with a Bruker DRX-500 spectrometer operating at 500 MHz. The sample solutions of the block copolymer at a polymer concentration (C_p) of 5.0 mg cm^{-3} for ^{1}H NMR measurements were prepared in D_2O and DMSO-d_6. Chemical shifts for ^{1}H NMR in D_2O were determined by using 3-(trimethylsilyl)propionic-2,2,3,3-d_4 acid as an internal reference.

Fluorescence. Fluorescence spectra were recorded on a Hitachi F-2500 fluorescence spectrophotometer. Sample solutions were prepared by mixing aliquots of stock solutions of the polymer and ANS (2.0×10^{-5} M) in aqueous 0.1 M NaCl solutions. The sample solutions were excited at 350 nm. Excitation and emission slit widths on the spectrometer were maintained at 20 and 5.0 nm, respectively.

Light scattering. Dynamic light scattering (DLS) and static light scattering (SLS) data were obtained at 25 °C with an Otsuka Electronics Photal DLS-7000DL light scattering photometer equipped with an ALV-5000E multi-τ digital time correlator. An Ar^+ laser (30.0 mW at 488 nm) was used as a light source. Sample solutions for DLS and SLS measurements were filtered with a 0.45 μm pore size membrane filter.

To obtain the relaxation time distribution by QELS, $\tau A(\tau)$, the inverse Laplace transform (ILT) analysis was performed using the algorithm REPES.[28–30]

$$g^{(1)}(t) = \int \tau A(\tau) \exp(-t/\tau) \mathrm{d}\ln \tau \quad (1)$$

Here τ is the relaxation time and $g^{(1)}(t)$ is the normalized autocorrelation function. The relaxation time distribution is given as a $\tau A(\tau)$ *versus* log τ profile. The relaxation rate, Γ ($=\tau^{-1}$), is a function of C_p and the scattering angle (θ).[31] The diffusion coefficient (D) is calculated from $D = (\Gamma/q^2)_{q\to 0}$, where $q = (4\pi n/\lambda)\sin(\theta/2)$ with n being the refractive index of the solvent and λ being the wavelength (=488 nm). The translational diffusion coefficient at limiting dilution (D_0) is calculated from

$$D = D_0(1 + k_d C_p) \quad (2)$$

where k_d is the hydrodynamic virial coefficient. The hydrodynamic radius (R_h) is calculated using the Einstein–Stokes relation $R_h = k_B T/6\pi\eta D_0$, where k_B is Boltzmann's constant, T is the absolute temperature, and η is the solvent viscosity.[32,33]

The weight-average molecular weight (M_w), z-average radius of gyration (R_g), and second virial coefficient (A_2) values were estimated from the relation[34]

$$\frac{KC_p}{R_\theta} = \frac{1}{M_w}\left(1 + \frac{1}{3}\langle R_g^2\rangle q^2\right) + 2A_2C_p \quad (3)$$

where R_θ is the Rayleigh ratio, $K = 4\pi^2 n^2 (\mathrm{d}n/\mathrm{d}C_p)^2/N_A\lambda^4$ with $\mathrm{d}n/\mathrm{d}C_p$ being the refractive index increment against C_p and N_A being Avogadro's number. By measuring R_θ for a set of C_p and θ, values of M_w, R_g, and A_2 were estimated from Zimm plots. Toluene was used for the calibration of the instrument. Values of $\mathrm{d}n/\mathrm{d}C_p$ were determined with an Otsuka Electronics Photal DRM-1020 differential refractometer at a wavelength of 488 nm at 25 °C.

TEM images. TEM images were taken on a Hitachi H-7000 microscope operating at 100 kV. The samples were stained with a 3% uranyl acetate solution.

Results and discussion

The conversion of G2 in the presence of PAMPS macro-CTA (M_w (SLS) = 2.21×10^4, M_w/M_n (GPC) = 1.28) was estimated to be 6.3% from ^{1}H NMR of the obtained block copolymer. The low conversion of G2 may be attributed to the steric hindrance of the bulky pendent dendritic groups of the monomer. Number-average degrees of polymerization (DP_n) for the PAMPS and PG2 block sequences in the obtained diblock copolymer were determined to be 71 and 3, respectively, on the basis of SLS and ^{1}H NMR data. The M_w/M_n value for the diblock copolymer determined from GPC analysis was 1.25, suggesting that the polymerization proceeded in accordance with a "living" fashion. The amphiphilic diblock copolymer obtained is soluble in water. We also prepared a diblock copolymer with the different block lengths using relatively smaller molecular weight PAMPS macro-CTA (M_w (SLS) = 4.29×10^3, M_w/M_n (GPC) = 1.18).

Values of DP_n for the PAMPS and PG2 blocks were 19 and 3, respectively, with an M_w/M_n value of 1.15 for the diblock copolymer. This block copolymer was insoluble in water. Therefore, we investigated the association behavior of PAMPS-*b*-PG2 where DP_n values for the PAMPS and PG2 blocks were 71 and 3, respectively. The molecular characteristics of the diblock copolymer are presented in Table 1.

Fig. 2 compares ^{1}H NMR spectrum of PAMPS-*b*-PG2 in D_2O at 27 °C with that in DMSO-d_6 at 100 °C. In D_2O, ^{1}H NMR spectrum of PAMPS-*b*-PG2 is almost the same as that of the PAMPS macro-CTA (PAMPS homopolymer). The resonance bands observed at 1.2–1.8 ppm are attributed to the pendent methyl protons and the methylene protons of the main chain, bands at 1.9–2.4 ppm to the methine proton of the main chain, bands at 3.1–3.7 ppm to the pendent methylene protons, and bands at 7.1–7.8 ppm to the amide proton. The resonance bands due to the PG2 block were not discernible, suggesting the hydrophobic association of PG2 in water. On the other hand, in DMSO-d_6 at 100 °C, the resonance bands related to PG2 were clearly observed at 4.8–5.2 and 6.5–6.8 ppm. The DP_n value for the PG2 block is 3, which was calculated from the integral area intensity ratio of the ^{1}H NMR resonance band for the pendent methylene protons in the AMPS unit and that for the benzyl protons in the G2 unit in DMSO-d_6 at 100 °C.

The fluorescence spectra of the ANS probe depend on microscopic polarity around the probe.[35–38] ANS emits fluorescence around 510 nm weakly in hydrophilic media, *e.g.*, in water but strongly in hydrophobic media accompanying a significant

Table 1 Molecular characteristics of PAMPS and PAMPS-*b*-PG2

	PAMPS	PAMPS-*b*-PG2
M_n (GPC)[a]	4.88×10^3	5.04×10^3
M_w/M_n (GPC)[a]	1.28	1.25
M_n (NMR)[b]	—	2.49×10^4
M_w (SLS)[c]	2.21×10^4	2.60×10^6
$\mathrm{d}n/\mathrm{d}C_p$[d]/cm^3 g^{-1}	0.153	0.160
A_2[c]/cm^3 g^{-2} mol	3.08×10^{-3}	1.04×10^{-5}
R_h[e]/nm	3.52	32.5
R_g[c]/nm	—	26.2
R_g/R_h	—	0.804
N_{agg}[f]	—	104

[a] Determined at 40 °C in methanol containing 0.2 M $LiClO_4$ by GPC relative to standard poly(ethylene oxide) (PEO). [b] Estimated from ^{1}H NMR in DMSO-d_6 at 100 °C along with M_w (SLS). [c] Determined at 25 °C in 0.1 M NaCl by static light scattering (SLS). [d] Determined at 488 nm. [e] Determined at 25 °C in 0.1 M NaCl by dynamic light scattering (DLS). [f] Calculated from a ratio of M_w (SLS) and M_n (NMR).

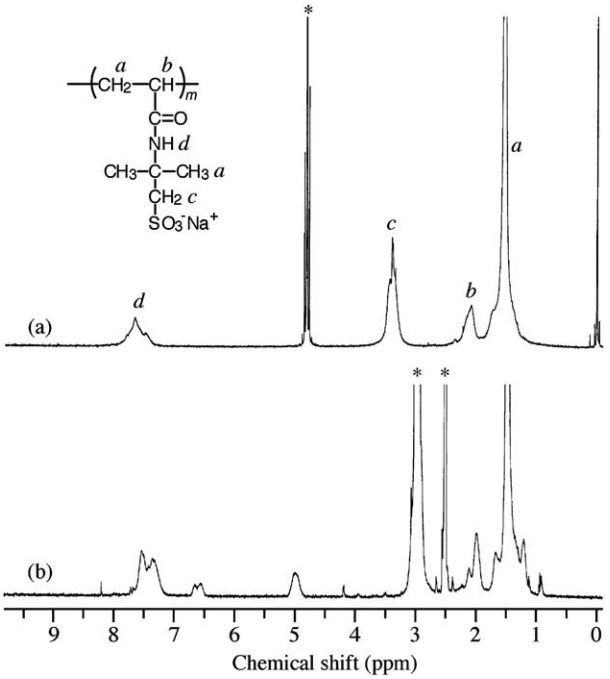

Fig. 2 Comparison of 500 MHz ^{1}H NMR spectra of PAMPS-*b*-PG2 in D_2O containing 0.1 M NaCl at 25 °C (a) and in DMSO-d_6 at 100 °C (b). The polymer concentration is 5.0 mg cm^{-3}. Asterisks represent solvent bands.

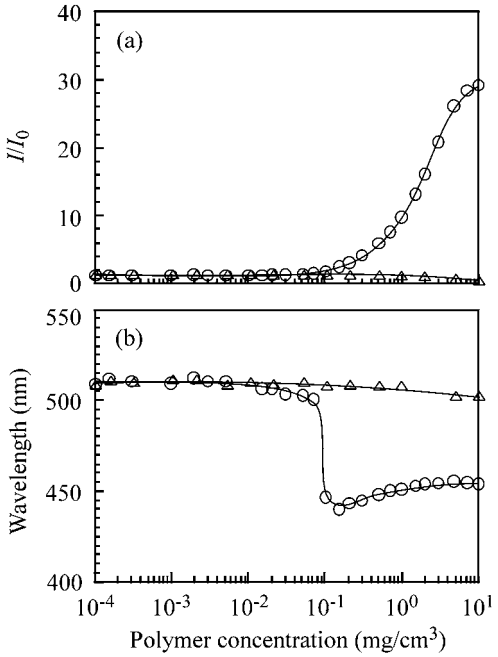

Fig. 3 Relative fluorescence intensity (I/I_0) (a) and emission maxima (b) in fluorescence spectra of 8-anilino-1-naphthalenesulfonic acid, ammonium salt hydrate (ANS) (2.0×10^{-5} M) as a function of concentrations of PAMPS (△) and PAMPS-*b*-PG2 (○) in aqueous 0.1 M NaCl solutions.

blue shift. Therefore, increased fluorescence intensity along with a blue shift of the emission maximum indicates that the probe is located in hydrophobic media.

The relative fluorescence intensity (I/I_0) of an emission band of ANS (2.0×10^{-5} M) solubilized in aqueous 0.1 M NaCl solutions is plotted against polymer concentration (C_p) in Fig. 3a, where I and I_0 are the fluorescence intensities in the presence and absence of the polymer, respectively. The I/I_0 ratios of PAMPS are constant around 1.0 in the whole range of C_p studied. In the case of PAMPS-*b*-PG2, the I/I_0 ratios are around 1.0 at $C_p \leq 0.07$ mg cm^{-3}. As C_p is increased, the I/I_0 ratios begin to increase at $C_p > 0.07$ mg cm^{-3}. These observations suggest that the polymer aggregates are able to incorporate ANS molecules into the hydrophobic microdomain formed from the association of the PG2 blocks.

Fig. 3b shows the C_p dependence of the ANS emission maximum wavelengths in the presence of PAMPS and PAMPS-*b*-PG2. The maximum wavelength for PAMPS is nearly constant at *ca.* 508 nm independent of C_p over the whole range of C_p depicted in Fig. 2b, which indicates the ANS probes existing in the bulk water phase. On the other hand, the maximum wavelengths in the presence of PAMPS-*b*-PG2 are constant at 508 nm in a low C_p region ($C_p < 0.07$ mg cm^{-3}), however the emission maxima begin to decrease in the C_p region of 0.07–1.0 mg cm^{-3} with increasing C_p, reaching a blue-shifted wavelength around 450 nm at higher C_p. This blue shift suggests the formation of hydrophobic microdomains, in which ANS probes are solubilized when C_p is higher than 1.0 mg cm^{-3}. A polymer concentration at the onset of the increase in I/I_0 (Fig. 3a) agrees with that at the onset of the blue shift of the emission maximum (Fig. 3b).

Fig. 4a compares DLS relaxation time distributions for PAMPS and PAMPS-*b*-PG2 at $C_p = 5.0$ mg cm^{-3} in aqueous 0.1 M NaCl solutions at a fixed θ of 90°. These polymers exhibit unimodal distributions with different relaxation times. The relaxation time (τ) at the peak top of the distribution for PAMPS-*b*-PG2 is longer than that of PAMPS.

In Fig. 4b, the relaxation rates ($\Gamma = \tau^{-1}$) for PAMPS and PAMPS-*b*-PG2 at $C_p = 5.0$ mg cm^{-3} estimated from DLS data at different measuring angles are plotted as a function of the square of the scattering vector (q^2). The linear relationship passing through the origin indicates that all the relaxation modes are due to translational diffusion. The diffusion coefficients (D) estimated from the slope of the Γ–q^2 plot for PAMPS andPAMPS-*b*-PG2 at $C_p = 5.0$ mg cm^{-3} are 8.71×10^{-7} and 7.34×10^{-8} cm^2 s^{-1}, respectively.

The D values for PAMPS increase with an increase in C_p (Fig. 4c), being a normal tendency for simple polyelectrolytes.[39–41] In contrast, the D values for PAMPS-*b*-PG2 are practically constant independent of C_p in the whole range of C_p studied (Fig. 4c). Therefore, the hydrodynamic virial coefficient (k_d) in eqn (2) can be regarded as virtually zero. No further aggregation between the polymer aggregates was recognized upon further increase in the polymer concentration beyond the C_p range shown in Fig. 3c. Consequently, the hydrodynamic size of the polymer aggregates, and hence the aggregation number (N_{agg}), is constant over a wide range of the polymer concentrations. Values of the hydrodynamic radii (R_h) can be calculated from the Stokes–Einstein relation along with the translational diffusion coefficient at limiting dilution (D_0) determined by the extrapolation of C_p to zero in D–C_p plots. Values of R_h for PAMPS and PAMPS-*b*-PG2 thus estimated are listed in Table 1.

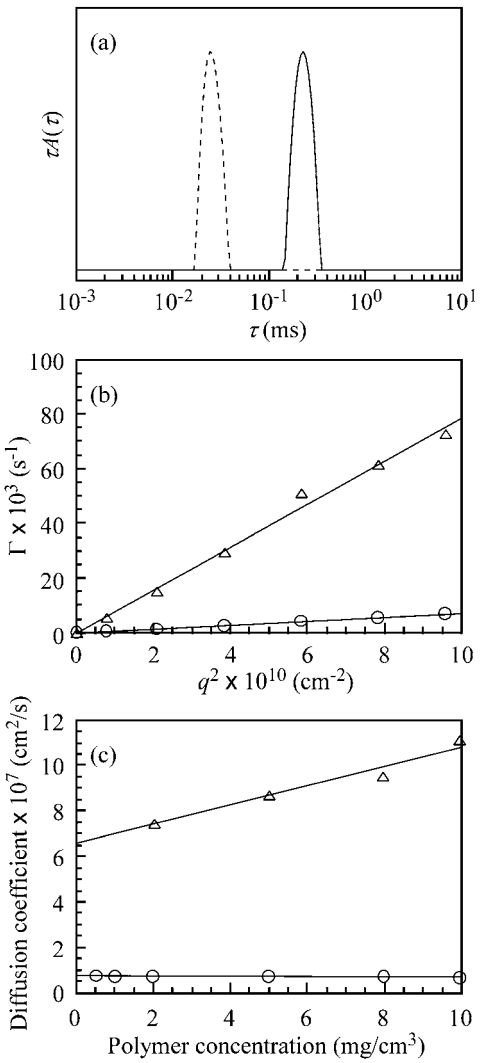

Fig. 4 (a) Typical examples of dynamic light scattering (DLS) relaxation time distributions for PAMPS (---) and PAMPS-*b*-PG2 (—) in 0.1 M NaCl aqueous solutions at 25 °C, where the polymer concentration (C_p) is 5.0 mg cm^{-3}. (b) Relationship between the relaxation rate (Γ) and the square of the scattering vector (q^2) for PAMPS (△) and PAMPS-*b*-PG2 (○) in aqueous 0.1 M NaCl solutions at C_p = 5.0 mg cm^{-3}. (c) Plots of the diffusion coefficient (D) for PAMPS (△) and PAMPS-*b*-PG2 (○) in aqueous 0.1 M NaCl solutions at 25 °C as a function of C_p at a scattering angle (θ) of 90°.

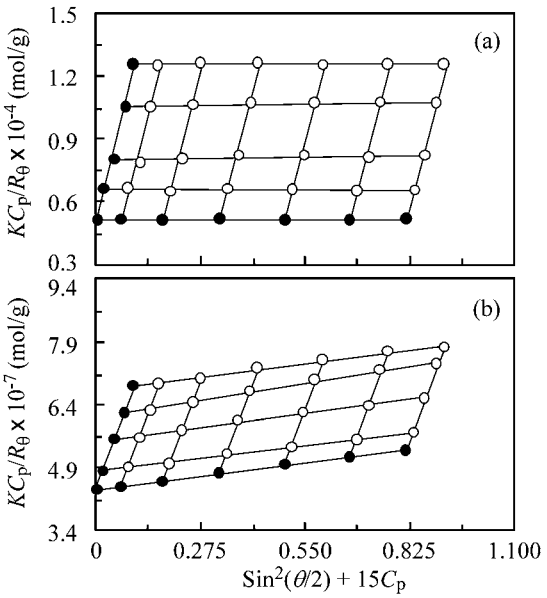

Fig. 5 Zimm plots at 25 °C for PAMPS (a) and PAMPS-*b*-PG2 (b) in aqueous 0.1 M NaCl solutions at scattering angles from 30° to 130° with a 20° interval. The polymer concentrations were varied from 2.0 to 10 mg cm^{-3}.

Fig. 5 compares Zimm plots for PAMPS and PAMPS-*b*-PG2 in aqueous 0.1 M NaCl solutions. The measurements of SLS were performed in a 2.0–10 mg cm^{-3} range of C_p. Values of dn/dC_p for PAMPS and PAMPS-*b*-PG2 at 488 nm are listed in Table 1. The M_w values are estimated by the extrapolation of θ and C_p to zero, and values of R_g and A_2 are estimated from the slope of the angular and concentration dependence in the Zimm plots, respectively. The SLS data for PAMPS and PAMPS-*b*-PG2 are presented in Table 1. The M_w value for PAMPS-*b*-PG2 is much lager than that for PAMPS, indicative of the multi-polymer aggregates of the PG2 blocks. The N_{agg} value of the PAMPS-*b*-PG2 aggregate was calculated from the ratio of the apparent M_w values of the polymer aggregate and a single polymer chain. The former was estimated from M_w and M_w/M_n determined by SLS and GPC, respectively. The molecular weight of the single polymer chain of PAMPS-*b*-PG2 was calculated from ^{1}H NMR spectra measured in DMSO-d_6 at 100 °C. The N_{agg} value thus estimated for PAMPS-*b*-PG2 is 104 (Table 1). Unfortunately, the R_g value for PAMPS was unable to be determined with SLS measurements, because angular dependence in the Zimm plot was too small to determine the value of R_g (<10 nm). The A_2 values for PAMPS and PAMPS-*b*-PG2 were estimated to be 3.08 × 10^{-3} and 1.04 × 10^{-5} cm^3 g^{-2} mol, respectively. Amphiphilic polyelectrolyte aggregates often exhibit a small A_2 value owing to an electrostatic shielding effect by counter ions condensed on the aggregates.[42,43]

The R_g/R_h ratio (ρ) is an important parameter that reflects a particle size distribution and conformation. The theoretical value of the ρ parameter for a homogeneous hard sphere is 0.788, and it increases substantially for less dense structures and polydisperse systems, *e.g.*, ρ = 1.5–1.7 for flexible linear chains in a good solvent while $\rho \geq 2$ for a rigid rod.[44–47] The ρ value for PAMPS-*b*-PG2 was found to be 0.804 (Table 1).

Fig. 6 shows a TEM image of the PAMPS-*b*-PG2 aggregates. Spheres with radii ranging 27–31 nm are observed. The size observed by TEM is almost the same as that estimated from light scattering measurements.

Assuming that the diblock copolymer forms a core–shell type polymer micelle with a core formed from the hydrophobic PG2 blocks and a shell formed from permanently charged PAMPS blocks, the R_h value is the sum of the radius of the core (R_c) and the corona thickness (L). The R_c can be calculated from eqn (4):[48,49]

$$R_c = [3M_{w,mic}w_{G2}/(4\pi N_A\rho_{G2}x_{G2})]^{1/3} \quad (4)$$

where $M_{w,mic}$ is the weight-average molecular weight of the micelle, w_{G2} is the weight fraction of the PG2 block in the diblock copolymer, N_A is Avogadro's number, ρ_{G2} is the density of G2,

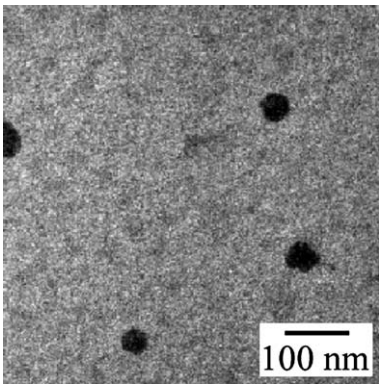

Fig. 6 TEM photograph of the PAMPS-*b*-PG2 aggregates.

and x_{G2} is the volume fraction of PG in the core of micelle. Using the values of $\rho_{G2} = 1.0$ mg cm^{-3} (assumed to be that of the G2 monomer) and $x_{G2} = 1.0$, R_c can be determined. The L value can also be calculated from the difference of R_h and R_c. These R_c and L values for the block copolymer micelle are 5.3 and 27.2 nm, respectively. The length of a full stretched PAMPS block is about 10.9 nm, based on DP$_n$ is 71 and 0.153 nm per monomeric unit. It should be noted that the length of shell L is larger than that of a stretched NaAMPS block with DP$_n$ = 71, which indicated that PAMPS-*b*-PG2 cannot form a simply core–shell micelle with a core formed by the PG2 blocks and a shell formed by PAMPS blocks in water. These results lead us to conclude that PAMPS-*b*-PG2 may form narrow polydispersity ellipsoidal micelles or multiple aggregates due to inter-micellar association of the spherical core–corona micelles.

Conclusions

The use of PAMPS macro-CTA allowed the synthesis of the novel amphiphilic diblock copolymer with a linear PAMPS block and a hydrophobic block bearing pendent dendritic moieties. It was suggested that production of PAMPS-*b*-PG2 with relatively low molecular weight distribution (M_w/M_n = 1.25) comes from the living nature of the polymerization process. In water, the amphiphilic nature of the amphiphilic diblock copolymer enabled to form aggregates. The motion of the bulky dendritic moieties was restricted because of hydrophobic association in water. Fluorescence data indicated that the hydrophobic microdomain could incorporate hydrophobic molecules such as ANS. The hydrodynamic radius of the polymer aggregate was 32.5 nm with a narrow unimodal distribution. The value of ρ parameter suggested that the polymer aggregates were nearly uniform. Further research of application of the PAMPS-*b*-PG2 aggregates to encapsulate hydrophobic molecules such as drugs is ongoing. The large degree of vacancies in the interior of dendrons can provide the ability to encapsulate many guest molecules. Furthermore, the terminal groups of dendrons can be modified with various functional groups.

Acknowledgements

This work was supported by Grant-in-Aid for Scientific Research on Innovative Areas "Molecular Soft-Interface Science" from the Ministry of Education, Culture, Sports, Science and Technology of Japan.

References

1 *Encyclopedia of Polymer Science and Engineering*, ed. H. F. Mark, N. M. Bikales, C. G. Overberger and G. Menges, Wiley, New York, 1985.
2 G. Kown, S. Suwa, M. Yokoyama, T. Okano, Y. Sakurai and K. Kataoka, *J. Controlled Release*, 1994, **29**, 17–23.
3 Y. Nagasaki, T. Okada, C. Scholz, M. Iijima, M. Kato and K. Kataoka, *Macromolecules*, 1998, **31**, 1473–1479.
4 A. Rolland, J. O'Mullane, L. Brookman and K. Petrak, *J. Appl. Polym. Sci.*, 1992, **44**, 1195–1203.
5 P. N. Hurter and T. A. Hatton, *Langmuir*, 1992, **8**, 1291–1299.
6 A. Kitahara, *Adv. Colloid Interface Sci.*, 1980, **12**, 109–140.
7 J. Issberner, R. Moors and F. Vögtle, *Angew. Chem., Int. Ed. Engl.*, 1994, **33**, 2413–2420.
8 D. A. Tomalia and P. R. Dvornic, *Nature*, 1994, **372**, 617–618.
9 Y. M. Chen, C. F. Chen, W. H. Liu, Y. F. Li and F. Xi, *Macromol. Rapid Commun.*, 1996, **17**, 401–407.
10 E. R. Zubarev and S. I. Stupp, *J. Am. Chem. Soc.*, 2002, **124**, 5762–5773.
11 J. M. J. Fréchet, *Science*, 1994, **263**, 1710–1715.
12 I. Gitsov, K. L. Wooley and J. M. J. Fréchet, *Angew. Chem., Int. Ed. Engl.*, 1992, **31**, 1200–1202.
13 I. Gitsov and J. M. J. Fréchet, *Macromolecules*, 1993, **26**, 6536–6546.
14 T. Imae, in *Structure–Performance Relationship in Surfactants*, ed. K. Esumi and M. Ueno, CRC Press, 2nd edn, 2003.
15 M. K. Georges, P. M. Veregin, P. M. Kazmaier and G. K. Hamer, *Macromolecules*, 1993, **26**, 2987–2988.
16 M. Kato, M. Kamigaito, M. Sawamoto and T. Higashimura, *Macromolecules*, 1995, **28**, 1721–1723.
17 J. S. Wang and K. Matyjaszewski, *Macromolecules*, 1995, **28**, 7572–7573.
18 J. Chiefari, Y. K. Chong, F. Ercole, J. Krstina, T. P. Le, R. T. A. Mayadunne, G. F. Meijs, G. Moad, C. L. Moad, E. Rizzardo and S. H. Thang, *Macromolecules*, 1998, **31**, 5559–5562.
19 K. Matyjaszewski, T. Shigemoto, J. M. J. Fréchet and M. R. Leduc, *Macromolecules*, 1996, **29**, 4167–4171.
20 M. R. Leduc, C. J. Hawker, J. Dao and J. M. J. Fréchet, *J. Am. Chem. Soc.*, 1996, **118**, 11111–11118.
21 B. S. Sumerlin, A. B. Lowe, D. B. Thomas and C. L. McCormick, *Macromolecules*, 2003, **36**, 1436–1439.
22 B. Ray, Y. Isobe, K. Morioka, S. Habaue, Y. Okamoto, M. Kamigaito and M. Sawamoto, *Macromolecules*, 2003, **36**, 543–545.
23 M. Arotçaréna, B. Heise, S. Ishaya and A. Laschewsky, *J. Am. Chem. Soc.*, 2002, **124**, 3787–3793.
24 J. F. Lutz, D. Neugebauer and K. Matyjaszewski, *J. Am. Chem. Soc.*, 2003, **125**, 6986–6993.
25 Y. Mitsukami, M. S. Donovan, A. B. Lowe and C. L. McCormick, *Macromolecules*, 2001, **34**, 2248–2256.
26 S. Yusa, Y. Shimada, Y. Mitsukami, T. Yamamoto and Y. Morishima, *Macromolecules*, 2003, **36**, 4208–4215.
27 K. W. Yeoh, C. H. Chew, L. M. Gan, L. L. Koh and H. H. Teo, *J. Macromol. Sci., Part A: Pure Appl. Chem.*, 1989, **26**, 663–680.
28 J. Jakes, *Czech. J. Phys.*, 1988, **B38**, 1305–1316.
29 K. Schillén, W. Brown and R. M. Johnsen, *Macromolecules*, 1994, **27**, 4825–4832.
30 W. Brown, K. Schillén, M. Almgren, S. Hvidt and P. Bahadur, *J. Phys. Chem.*, 1991, **95**, 1850–1858.
31 W. H. Stockmayer and M. Schmidt, *Pure Appl. Chem.*, 1982, **54**, 407–414.
32 *Dynamic Light Scattering*, ed. R. Pecora and J. Berne, Plenum Press, New York, 1976.
33 *Laser Light Scattering*, ed. B. Chu, Academic Press, New York, 2nd edn, 1991.
34 B. H. Zimm, *J. Chem. Phys.*, 1948, **16**, 1099–1116.
35 J. Slavik, *Biochim. Biophys. Acta*, 1982, **694**, 1–25.
36 A. H. Hunt and B. Jirgensons, *Biochemistry*, 1973, **12**, 4435–4441.
37 G. Weber and L. B. Young, *J. Biol. Chem.*, 1964, **239**, 1415–1423.
38 L. Stryer, *J. Mol. Biol.*, 1965, **13**, 482–495.
39 W. Peiqiang, M. Siddiq, C. Huiying, Q. Di and C. Wu, *Macromolecules*, 1996, **29**, 277–281.

40 S. Yusa, M. Kamachi and Y. Morishima, *Macromolecules*, 2000, **33**, 1224–1231.
41 J. Fundin, W. Brown and M. S. Vethamuthu, *Macromolecules*, 1996, **29**, 1195–1203.
42 J. R. Quintana, M. D. Jánez, M. Villacampa and I. Katime, *Macromolecules*, 1995, **28**, 4139–4143.
43 M. Villacampa, E. D. Apodaca, J. R. Quintana and I. Katime, *Macromolecules*, 1995, **28**, 4144–4149.
44 E. Nordmeier and M. D. Lechner, *Polym. J.*, 1989, **21**, 623–632.
45 T. Konishi, T. Yoshizaki and H. Yamakawa, *Macromolecules*, 1991, **24**, 5614–5622.
46 A. Qin, M. Tian, C. Ramireddy, S. E. Webber, P. Munk and Z. Tuzar, *Macromolecules*, 1994, **27**, 120–126.
47 *Modern Theory of Polymer Solutions*, ed. H. Yamakawa, Harper & Row, New York, 1971.
48 S. Pispas, R. Hadjichristidis, I. Potemkin and A. Khokhlov, *Macromolecules*, 2000, **33**, 1741–1746.
49 S. Keki, G. Deak, A. Kuki and M. Zsuga, *Polymer*, 1998, **39**, 6053–6055.